

Activation of Human Cerebral and Cerebellar Cortex by Auditory Stimulation at 40 Hz

Maria A. Pastor,¹ Julio Artieda,¹ Javier Arbizu,² Josep M. Marti-Climent,² Ivan Peñuelas,² and Jose C. Masdeu¹

Departments of ¹Neurology and ²Nuclear Medicine, University of Navarra School of Medicine, 31080 Pamplona, Spain

We used functional brain imaging with positron emission tomography (PET)-H₂ ¹⁵O to study a remarkable neurophysiological finding in the normal brain. Auditory stimulation at various frequencies in the gamma range elicits a steady-state scalp electroencephalographic (EEG) response that peaks in amplitude at 40 Hz, with smaller amplitudes at lower and higher stimulation frequencies. We confirmed this finding in 28 healthy subjects, each studied with monaural trains of stimuli at 12 different stimulation rates (12, 20, 30, 32, 35, 37.5, 40, 42.5, 45, 47.5, 50, and 60 Hz). There is disagreement as to whether the peak in the amplitude of the EEG response at 40 Hz corresponds simply to a superimposition of middle latency auditory evoked potentials, neuronal synchronization, or increased cortical synaptic activity at this stimulation frequency. To clarify this

issue, we measured regional cerebral blood flow (rCBF) with PET-H₂ ¹⁵O in nine normal subjects at rest and during auditory stimulation at four different frequencies (12, 32, 40, and 47 Hz) and analyzed the results with statistical parametric mapping. The behavior of the rCBF response was similar to the steady-state EEG response, reaching a peak at 40 Hz. This finding suggests that the steady-state amplitude peak is related to increased cortical synaptic activity. Additionally, we found that, compared with other stimulation frequencies, 40 Hz selectively activated the auditory region of the pontocerebellum, a brain structure with important roles in cortical inhibition and timing.

Key words: steady-state auditory evoked potentials; gamma oscillatory activity; regional cerebral blood flow; positron emission tomography; cerebellum; auditory cortex

In humans, auditory stimulation at different gamma frequencies elicits an electroencephalographic (EEG) steady-state response (SSR) that cycles at the stimulation frequency and has the greatest amplitude when the stimulus is given at 40 Hz (Galambos et al., 1981). Lower or higher frequencies produce a response of smaller amplitude. These oscillatory responses seem to be generated at the level of the auditory cortex, although modulated by thalamocortical systems (Makela and Hari, 1987; Steriade et al., 1991). The significance and origin of the steady-state potentials continue to be debated (Basar et al., 1987; Santarelli et al., 1995; Gutschalk et al., 1999). It is unclear whether the power increment of the steady-state auditory response at 40 Hz results merely from the temporal coherence (phase summation) of “middle latency” evoked responses, phase synchronization of a pool of cortical neurons, or a true increase in cortical synaptic activity at 40 Hz. Synaptic activity causes an increment in regional cerebral blood flow (rCBF). To test the hypothesis that the enhanced response at 40 Hz reflects increased synaptic cortical activity, we measured rCBF with positron emission tomography (PET) in the auditory cortex and other brain regions during auditory stimulation at different frequencies. A rise in rCBF at 40 Hz stimulation would suggest that the enhanced EEG response corresponds to increased synaptic activity at this frequency.

Most studies of oscillatory behavior have concentrated on the activity of the cortex and thalamus. PET allowed us to study the effect of gamma frequency stimulation on other brain structures, to test a second hypothesis: namely, that given the singular behavior of the EEG response to auditory stimulation at 40 Hz, brain regions outside the auditory cortex are activated specifically by stimulation at 40 Hz and not at other gamma frequencies.

MATERIALS AND METHODS

Subjects. We studied 28 normal volunteers (16 females; 12 males; mean age = 35.3; SD = 4.2) who had no history of audiological or neurological disease and had normal general and neurological examinations. All subjects were right handed according to the Edinburgh Handedness Inventory (Oldfield, 1971). The protocol was approved by the Ethics Committee of the University Hospital, and all subjects gave their written informed consent for the study, according to the declaration of Helsinki, after its nature was fully explained to them.

Neurophysiological study. Steady-state, auditory-evoked potentials during wakefulness were recorded at 21 scalp locations (10–20 EEG international system); all referred to a binaural reference. Electrode impedance was kept at <5000 Ω. The stimuli were click applied monaurally to the right ear at the suprathreshold intensity of 80 dB HL (Picton et al., 1987) and at 12 different frequencies (12, 20, 30, 32.5, 35, 37.5, 40, 42.5, 45, 47.5, 50, and 60 Hz). Responses were bandpass filtered between 1 and 500 Hz. Five hundred responses, in epochs of 500 msec, were averaged for each stimulus frequency. At the 21 electrodes, a fast Fourier transform (FFT) was performed in each trial. The dominant frequencies of power spectra [stimulus rate locked responses (SRLRs)] were determined for all stimulation frequencies, and the amplitude (square root of power) was obtained at the 21 electrodes. All of the dominant peaks of frequency and harmonic and subharmonic responses were measured. In addition, for each stimulation frequency, we measured the 40 Hz component of the elicited response. This neurophysiological study identified F3 as the electrode where maximum amplitude steady-state evoked potentials were recorded, and therefore, we selected electrical activities at F3 to compare them with rCBF PET measurements (see Fig. 1).

PET procedure. In nine subjects of the group (four females; five males;

Received June 11, 2002; revised Sept. 6, 2002; accepted Sept. 23, 2002.

This work was supported by the University of Navarra Research Fund PIUNA 13298312 and the Spanish Ministerio de Educación y Cultura Dirección General de Investigación Científica y Técnica PB 92-0713. We thank Profs. David Brooks and Richard Wise for help with preliminary data analysis, Dr. John Ashburner for reviewing the methodological aspect of this study, and Prof. Karl Friston for his valuable suggestions on this manuscript.

Correspondence should be addressed to Dr. Maria A. Pastor, Department of Neurology, University of Navarra School of Medicine, Clínica Universitaria, 31080 Pamplona, Spain. E-mail: mapastor@unav.es.

Copyright © 2002 Society for Neuroscience 0270-6474/02/2210501-06\$15.00/0

mean age = 30.4; SD = 4.8), selected on the basis of availability and whose EEG data were no different from the entire group of 28 subjects, we measured rCBF with PET- $H_2^{15}O$ at rest and during auditory stimulation at four different frequencies: 12, 32, 40, and 47 Hz. The PET scans were performed with an ECAT EXACT HR+ (Siemens/CTI, Knoxville, TN) that collected 63 simultaneous parallel planes over a 15.2 cm axial field of view. The tomographic resolution was 4.5 mm. Transmission scanning was done before radiopharmaceutical injection using three ^{68}Ge rotating rod sources. The subject was positioned so that the entire intracranial volume, including the cerebellum, was included in the fields of view.

The subjects lay comfortably in a supine position. No attempt was made to control the subjects' thought content or attention. A small catheter was placed in the left cubital vein for the injection of the radioisotope. Auditory stimulation was performed through a mini-earphone introduced in the right external auditory canal. The left external auditory canal was occluded with a silicone stopper. Series of non-filtered clicks were applied monoaurally to the right ear, at 80 dB intensity. Each subject underwent five consecutive scans at 20 min intervals, one at rest and one for each frequency of auditory stimulation (12, 32, 40, and 47 Hz). The order of the different frequency stimulation and baseline scans was randomized across subjects to avoid an order effect. For the baseline scan, subjects lay quietly. After 60 sec at rest or listening to clicks, subjects received 370 MBq of $H_2^{15}O$ as an intravenous bolus. Scans were initiated automatically when the radioactive count rate in the brain reached a threshold value of 100 kcounts/sec, ~20 sec after intravenous injection, and continued for 60 sec. Emission data were corrected for attenuation by means of the transmission scan performed previously.

PET scans were analyzed using Statistical Parametric Mapping (SPM99; Wellcome Department of Cognitive Neurology, London, UK) (Friston et al., 1995b, 1996) on a Matlab 5.3 platform (MathWorks, Natick, MA). Head movement was corrected by rigid alignment (Friston et al., 1995a). The scans were then spatially normalized using the template from the Montreal Neurological Institute series and the reference system of Talairach and Tournoux (1988). The scans were smoothed using a Gaussian filter set at 10 mm full width at half-maximum in plane to increase the signal-to-noise ratio. Data were analyzed after construction of a design matrix for the analysis of group data for conditions and covariates. All scans were subjected to an analysis of covariance (ANCOVA). This procedure removes the confounding effect of differences in global activity across scans and normalizes global activity (measured as radioactive counts) to a notional mean rCBF of 50 ml · dl⁻¹ · min⁻¹. For each voxel, the ANCOVA generated five condition-specific mean rCBF values and associated error variances.

With SPM, we performed a cognitive subtraction, comparing the mean blood flow elicited by the different stimulation frequencies on a voxel-to-voxel basis. To make inferences about stimulus-frequency-dependent rCBF responses and thereby test our hypotheses, we specified a series of contrasts pertaining to the condition-specific effects, as follows: (1) we compared rCBF auditory-evoked responses across all frequencies relative to rest; we used the ensuing (T) statistical parametric map (from which we derived Z scores only for tabular reporting) to identify the auditory cortex region showing the greatest rCBF response. (2) To test the hypothesis that 40 Hz stimulation, compared with the other frequencies, may specifically activate regions other than the auditory cortex, we performed a second contrast comparing stimulation at 40 Hz with the group of the other repetitive stimulation frequencies; we used the ensuing (T) statistical parametric map to identify the cerebellar region showing the greatest rCBF response. (3) To assess the correlation between the EEG response and the rCBF activation at the voxels with the greatest activation, determined from the two previous contrasts (in the auditory area and cerebellum), we then specified a third contrast. Its weights were obtained by linear interpolation for the frequencies used in the PET experiment from the amplitude of the EEG SSRs, using the data presented in Figure 1B. The resulting four amplitudes were then mean corrected to a mean of 0, and the rest condition was discounted using a contrast weight of 0. The contrast testing the hypothesis that the EEG steady-state response could predict activation was 0, -0.8, 0.6, 2.1, and -1.9. It is important to note that this contrast is orthogonal with each of the two previous contrasts applied (1 and 2). In other words, the identification of the most responsive auditory voxel is independent of frequency-specific effects.

We used an uncorrected threshold of $p < 0.001$. Because our inferences were restricted to the cerebral and cerebellar auditory areas, this

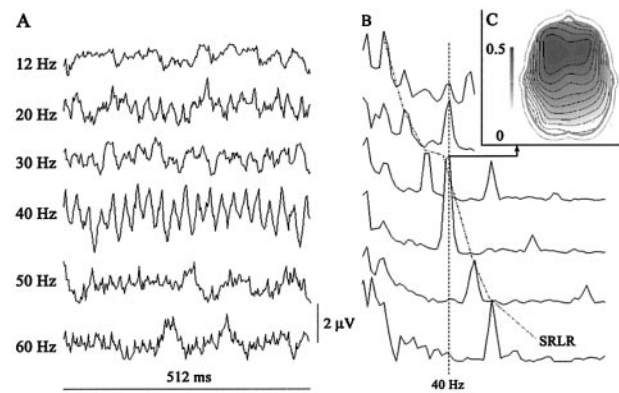


Figure 1. *A, B*, Electroencephalographic recording at electrode F3 of steady-state auditory potentials from a normal subject receiving auditory stimuli at the following frequencies: 12, 30, 40, 50, and 60 Hz. *A*, Steady-state responses; average of 500 trials. *B*, Grand average of steady-state fast Fourier transform at 12, 20, 30, 40, 50, and 60 Hz stimulation frequencies. Note the peaks at 40 Hz when the stimulation frequency was at one of its subharmonic rates, 10 and 20 Hz (40 Hz label), and the peaks at the rate of auditory stimulation (SRLR). *C*, EEG map showing the topography of the 40 Hz SRLR grand average of the entire experimental group.

corresponds to a threshold of $p < 0.05$ correcting for the volume of interest.

RESULTS

Neurophysiological study

The steady-state, auditory-evoked response, phase locked with the presented click frequency, was recorded at 12, 20, 30, 32.5, 35, 37.5, 40, 42.5, 45, 47.5, 50, and 60 Hz. As a result of a rapidly repeated auditory stimulus application, an initial transient response evolved into an oscillatory EEG response having the same frequency as the stimulus (SRLR). Figure 1*A* represents average recordings of the steady-state, auditory-evoked responses in a normal subject at the different frequencies. The oscillatory response reached the greatest amplitude at ~40 Hz and subsequently decreased at higher click rates. Figure 1*B* represents the grand average of steady-state fast FFTs at 12, 20, 30, 40, 50, and 60 Hz stimulation frequencies. The fast Fourier transforms analysis revealed three major components. A first component peaked at 10 Hz and had an occipital predominance. It is possibly related to EEG α activity. A second component peaked at the rate of auditory stimulation and was time locked with the stimulus rate (SRLR). Its amplitude (square root of the power) depended on the stimulation frequency, reaching a maximum at ~40 Hz (37.75; SD of 1.84) (Fig. 2). We extracted the mean value at 12, 32, 40, and 47 Hz for the group of nine subjects who had PET to compare them with rCBF values (12 Hz = 22.23; 32 Hz = 35.4; 40 Hz = 50.59; 47 Hz = 10.99). The third component was observed at 40 Hz when the stimulation frequency was at one of its subharmonic rates, 10 and 20 Hz.

Because we used binaural reference electrodes, the largest positive and negative potentials of the steady-state, auditory-evoked responses at 40 Hz were recorded in the frontal region contralateral to the side stimulated (at the F3 electrode with right ear stimulation) (Fig. 1*C*). For this reason, in all subjects, we chose the activity recorded at F3 to compare it with rCBF changes.

PET studies

Compared with rest, repetitive auditory stimulation of the right ear at 12, 32, 40, and 47 Hz elicited an increase in rCBF, shown

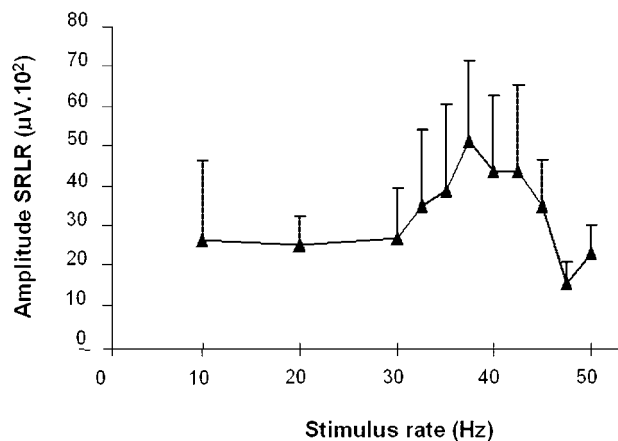


Figure 2. Effect of the auditory stimulation at different rates on the amplitude of the SRLR (grand average of 28 normal subjects). The amplitude (square root of the power of the fast Fourier transforms) of the SRLR reached a maximum at ~ 40 Hz (37.75; SD of 1.84). Error bars indicate SD.

on SPM(T) maps, in two larger areas: (1) contralateral auditory cortex (Heschl's gyrus) and (2) contralateral superior temporal gyrus and three smaller areas: (3) ipsilateral postcentral gyrus, (4) ipsilateral inferior temporal gyrus, and (5) ipsilateral posterior Sylvian area (Table 1, Fig. 3). A decrement in rCBF was observed at the head of the contralateral caudate nucleus and ipsilateral posterior cingulate cortex (Table 1, Fig. 3). The changes in rCBF in the auditory area followed a similar pattern to that of the EEG SRLRs at the different frequencies, with the highest activation at 40 Hz.

Compared with stimulation at other frequencies, 40 Hz stimulation elicited an increased rCBF in the cortex of the posterior aspect of both cerebellar hemispheres, predominantly on the side contralateral to auditory stimulation (Table 2, Fig. 4). The activated area, lateral to the paravermian region, was located on crus II using Schmahmann's nomenclature (Schmahmann et al., 1999). At the voxel maximally activated in these areas, rCBF clearly peaked during 40 Hz stimulation compared with other stimulation frequencies (Fig. 4).

In the third contrast, derived from the SRLR values, both the temporal auditory cortex and cerebellar auditory clusters showed a pattern of rCBF activation similar to that of the EEG SRLRs at the different frequencies, with the highest activation induced by 40 Hz. However, although all stimulation frequencies increased rCBF at the temporal cortex, stimulation frequencies other than 40 Hz actually depressed or failed to significantly change rCBF at the cerebellar clusters. The difference can be seen comparing Figure 3 (the parameter estimates at the temporal cortex cluster) with Figure 4 (the parameter estimates at the cerebellar clusters).

DISCUSSION

Neurophysiological study

The results of our electrophysiological study agree with those of Galambos et al. (1981) and Azzena et al. (1995). The SRLRs increased in amplitude in the 30–40 Hz range and decreased at rates of >40 Hz. The topography of the EEG steady-state response in our study, with greatest amplitude in contralateral frontal electrodes, is a standard finding when the recording is performed with balanced earlobe reference electrodes (Azzena et al., 1995; Maiste et al., 1995). Using a noncephalic reference,

the recordings show phase reversals in temporal regions (Johnson et al., 1988). This tangential dipole is better defined by magnetoencephalography (MEG) studies, which demonstrate the source in the primary auditory cortex, with a projection to central fields (Engelien et al., 2000). Because the amplitude of the EEG response obtained with our study design was greatest at F3, it seemed logical to use data from this electrode to compare them with rCBF data.

PET studies

For the study of auditory stimuli, PET has advantages compared with functional magnetic resonance imaging (fMRI). PET systems are quiet, whereas the radio frequency generators in MRI units produce noise that can reach 117 dB, thus masking study stimuli (Counter et al., 1997). Although PET systems do not have as much spatial resolution as MRI, their spatial resolution is superior to that of most neurophysiological systems and is not restricted to the study of cortical structures.

Auditory stimulation compared with baseline

Activated clusters were located in the contralateral primary and secondary auditory cortex, in the contralateral caudate nucleus, and in the ipsilateral posterior cingulate cortex. With the first contrast applied, all frequencies versus rest, the cerebellar hemispheres did not appear to be activated. However, only clusters of cerebellar activation appeared in the second contrast, when we compared 40 Hz versus the other stimulation frequencies. The difference between the results of the two contrasts is explained by the results of the third contrast. Both the temporal auditory cortex and the cerebellar auditory clusters showed a pattern of rCBF activation similar to that of the EEG SRLRs at the different frequencies, with the highest activation induced by 40 Hz. However, although all stimulation frequencies increased rCBF at the temporal cortex, stimulation frequencies other than 40 Hz actually depressed or failed to significantly change rCBF at the cerebellar clusters. Thus, the cerebellar cluster did not appear when the group of all frequencies was compared with rest, because the negative effect of some of the frequencies cancelled out the rCBF-enhancing effect of 40 Hz stimulation (compare Fig. 3 with Fig. 4).

Auditory cortex

We found an asymmetry in temporal lobe activation, with a larger rCBF increase in the region of the contralateral primary auditory cortex. Studies using monaural auditory stimulation have shown a strong contralateral temporal lobe activation (Hirano et al., 1997). We also found a second smaller activated area in the superior temporal gyrus, surrounding the primary auditory cortex. This area has been enhanced in studies using complex auditory patterns of stimulation, such as music or speech, suggesting that it may have a role in temporal auditory pattern detection (Creutzfeldt and Ojemann, 1989; Zatorre et al., 1992).

SSRs show maximum amplitude when tone pulses are presented at repetition rates near 40 Hz. To explain this finding, it has been postulated that the SSR consists of superimposed transient middle latency responses that display wave periods near 40 Hz and summate with one another when phase locked by 40 Hz steady-state stimulation. Some neurophysiological data, however, seemed to contradict this postulate. Using tones and MEG-recording techniques, Pantev et al. (1996) studied the cortical sources of the 40 Hz auditory steady-state fields (SSFs) and middle latency auditory-evoked potentials. They found that these

Table 1. Cerebral regions activated (rCBF) comparing the effect of grouping auditory repetitive stimulation at all frequencies versus the condition at rest

Type of rCBF change and area activated	<i>k</i>	<i>t</i>	<i>Z</i>	<i>p</i>	<i>x, y, z</i>
rCBF increment					
Contralateral auditory area (left)	515	9.38	5.96	<0.0001	−36, −26, 10
Contralateral superior temporal gyrus (left)	122	5.21	4.19	<0.0001	−64, −36, 8
Ipsilateral postcentral gyrus (right)	35	4.14	3.55	<0.0001	36, −24, 48
Ipsilateral inferior temporal gyrus (right)	31	3.99	3.44	<0.0001	46, −30, −20
Ipsilateral posterior Sylvian area (right)	21	4.47	3.75	<0.0001	36, −10, 18
rCBF decrement					
Contralateral caudate (left)	111	4.45	3.74	<0.0001	−4, 8, 0
Ipsilateral posterior cingulate cortex (right)	77	5.56	4.38	<0.0001	10, −34, 28

Data include cluster size (*k*), *t* statistic, *Z* scores, uncorrected significance level (*p*), and the coordinates of the cluster of activated voxels in standard stereotaxic space (Talairach and Tournoux, 1988) (*x, y, z*).

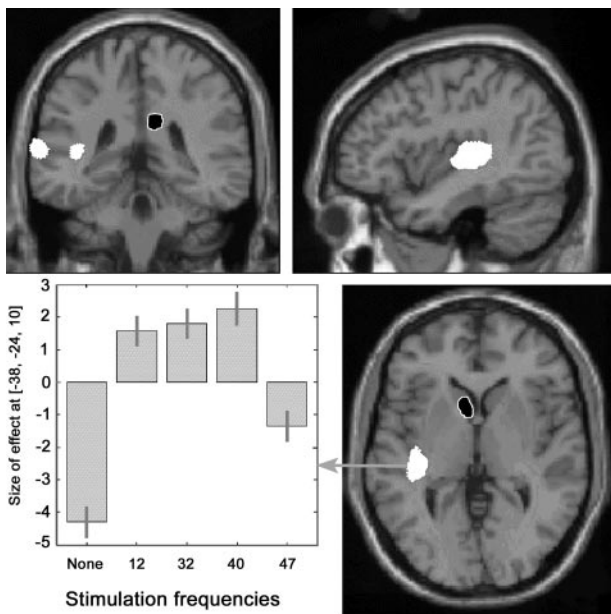


Figure 3. Anatomical location of areas with significant changes in rCBF during auditory stimulation (grouping of all frequencies compared with resting condition) projected on coronal, sagittal, and transverse sections of a T1-weighted canonical MRI of the human brain (increment in white and decrement in black with white margin). Data are given in Table 1. The chart depicts the size of the effect of the parameter estimates weighted by the amplitude of the EEG steady-state auditory responses in the voxel of greatest activation (*x*, −36; *y*, −26; *z*, 10) at rest and at each of the four stimulation frequencies.

two types of responses arise in different locations at the auditory area, suggesting a diverse origin for the 40 Hz SSF and entrained middle latency responses. However, direct evidence of increased temporal cortex synaptic activity specific to 40 Hz stimulation was lacking. We worked with the hypothesis that rCBF in the auditory area of the temporal lobe would follow a similar pattern to the amplitude of the electrical steady-state response, increasing as the stimulus rate climbed to 30–40 Hz and decreasing at higher rates. The results support our hypothesis: the rCBF in the voxel with the greatest activation of the cluster located in the auditory cortex increased at auditory stimulation rates from 12 to 40 Hz, decreasing at 47 Hz. This finding suggests that the enhanced EEG response to stimulation at 40 Hz is not just the result of increased neuronal synchronization but reflects an overall increase in auditory cortex synaptic activity at this frequency. Thus, our study

contributes to clarification of an ongoing controversy regarding the origin of the steady-state potentials (Basar et al., 1987; Santarelli et al., 1995; Gutschalk et al., 1999).

Region of the head of the left caudate nucleus and right posterior cingulate cortex

Compared with rest, repetitive auditory stimulation produced a significant decrement in rCBF at the head of the left caudate nucleus and right posterior cingulate cortex. The caudate is activated to a similar degree by auditory stimulation during wakefulness and non-rapid-eye-movement sleep (Portas et al., 2000). Thus, even a stimulation paradigm such as ours, not specifically requiring any attention or any other perceptual or cognitive effort, is likely to activate the caudate nucleus. There is ample evidence that this structure participates in the processing of more complex auditory tasks. For instance, target detection of auditory stimuli activates the caudate nuclei and posterior cingulate regions (Kiehl et al., 2001). Posterior cingulate gyrus activation has been described even with simple auditory stimulation paradigms, and a decrement in rCBF occurred with high-intensity stimuli, similarly to what happened in our study (Lockwood et al., 1999).

Activation by 40 Hz compared with other stimulation frequencies

Compared with stimulation at lower or higher frequencies, auditory stimulation at 40 Hz caused bilateral activation of the cerebellar hemispheres, with some contralateral dominance. The activated area was in the posterolateral portion of the hemisphere, lateral to the paravermian region, in crus II using Schmahmann's nomenclature (Schmahmann et al., 1999). A similar location in the cerebellum was activated in other PET studies exploring temporal auditory processing (Penhune et al., 1998; Lockwood et al., 1999; Griffiths, 2000; Ramnani et al., 2000). The anatomical coincidence emphasizes the important role of this cerebellar region in the processing of information related to auditory stimuli. This region differs from the vermicular and floccular areas that receive direct cochlear and collicular input. It corresponds to an area receiving auditory, visual, and somesthetic information. Connectivity studies, performed primarily in the cat and in rodents, have determined that the main bulk of afferents to this area originates in the temporal lobe and has a relay in the pontine nuclei before reaching the cerebellar cortex. In the primate, Schmahmann and Pandya (1991) found that projections from the primary auditory area are lacking. Instead, corticopontine auditory fibers originate in the second auditory area AII and adjacent

Table 2. Regions activated, in the cerebellar hemispheres, comparing stimulation at each frequency with the grouping of stimulation at the other frequencies (12, 32, 40, and 47 Hz)

Stimulation frequency	<i>k</i>	<i>t</i>	<i>Z</i>	<i>p</i>	<i>x</i> , <i>y</i> , <i>z</i>
12 Hz				NS	
32 Hz				NS	
40 Hz					
Contralateral cerebellar hemisphere (left)	54	3.95	3.41	0.0001	−30, −82, −42
Ipsilateral cerebellar hemisphere (right)	16	3.75	3.28	0.001	28, −80, −48
47 Hz				NS	

Data include cluster size (*k*), *t* statistic, *Z* scores, uncorrected significance level (*p*), and the coordinates of the cluster of activated voxels in standard stereotaxic space (Talairach and Tournoux, 1988) (*x*, *y*, *z*).

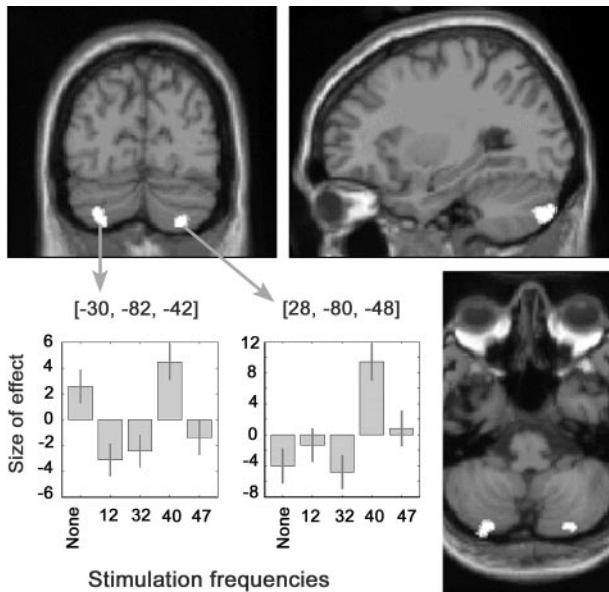


Figure 4. Regions with increased rCBF during 40 Hz auditory stimulation compared with stimulation at other frequencies. The activated areas, larger in the cerebellar hemisphere contralateral to the stimulated ear, are projected on a canonical image of the human brain obtained with T1-weighted MRI in the coronal, sagittal, and transverse planes. The chart depicts the effect size of the parameter estimates weighted for the amplitude of the EEG steady-state auditory response in the voxels of greatest activation (*x*, −30; *y*, −82; *z*, −42; and *x*, 28; *y*, −80; *z*, −48) at rest and during stimulation at each of the four frequencies. The left cerebellar hemisphere is on the *left* of the image.

association areas, but the most important bulk of corticoponto-cerebellar afferents is from multimodal areas in the upper bank of the superior temporal sulcus. These neurons project to the dorsolateral and lateral nuclei of the pons, which, in turn, project to the cerebellar area activated in our study (Brodal, 1979).

It could be argued that cerebellar activation by 40 Hz stimuli simply represents an enhancement of the spontaneous baseline frequency discharge of Purkinje neurons, from 30 to 50 Hz (Strahlendorf et al., 1984). Although possible, this explanation does not seem likely, because this baseline frequency is found in the Purkinje neurons of the entire cerebellar cortex and is not restricted to the area activated in our study. Examples include neurons placed more superiorly in the cerebellar hemisphere, with a somatosensory receptive field (Fu et al., 1997), floccular neurons processing vestibular–oculomotor interactions (Fukushima et al., 1999), or visually responsive Purkinje neurons located higher in the cerebellar hemisphere (Marple-Horvat et al., 1998).

To explain why auditory cortex was activated by all stimulation frequencies, whereas cerebellar activation was only detected comparing 40 Hz with the other frequencies, we could postulate that the cerebellum becomes more active to inhibit excessive cortical firing at some stimulation frequencies. For auditory stimuli, the critical stimulation frequency seems to be ~40 Hz. Perhaps, this is an indirect indication of the propensity of some brain regions to resonate at this frequency (Kapoor et al., 1991). Widespread cortical synchronization at the gamma band, ~40 Hz, may precede photically induced seizures (Parra et al., 2001). Other data suggest a cortical inhibitory role for the cerebellum. Small amplitude electrical stimulation of the cerebellar cortex in humans reduces cortical excitability (Ugawa et al., 1991). Some patients with cortical myoclonus have predominantly cerebellar pathology, suggesting that the enhanced cortical excitability may arise from deficient cerebellar control (Artieda and Obeso, 1993; Tijssen et al., 2000).

Both the neurophysiological studies confirmed by our data and the novel findings of auditory cortex synaptic activation and of specific cerebellar activation at 40 Hz suggest that this frequency plays a distinct role in the brain mechanisms involved in auditory processing.

REFERENCES

- Artieda J, Obeso JA (1993) The pathophysiology and pharmacology of photic cortical reflex myoclonus. *Ann Neurol* 34:175–184.
- Azzena GB, Conti G, Santarelli R, Ottaviani F, Paludetti G, Maurizi M (1995) Generation of human auditory steady-state responses (SSRs). I. Stimulus rate effects. *Hear Res* 83:1–8.
- Basar E, Rosen B, Basar-Eroglu C, Greitschus F (1987) The associations between 40 Hz-EEG and the middle latency response of the auditory evoked potential. *Int J Neurosci* 33:103–117.
- Brodal P (1979) The pontocerebellar projection in the rhesus monkey: an experimental study with retrograde axonal transport of horseradish peroxidase. *Neuroscience* 4:193–208.
- Counter SA, Olofsson A, Grahn HF, Borg E (1997) MRI acoustic noise: sound pressure and frequency analysis. *J Magn Reson Imaging* 7:606–611.
- Creutzfeldt O, Ojemann G (1989) Neuronal activity in the human lateral temporal lobe. III. Activity changes during music. *Exp Brain Res* 77:490–498.
- Engelien A, Schulz M, Ross B, Arolt V, Pantev C (2000) A combined functional in vivo measure for primary and secondary auditory cortices. *Hear Res* 148:153–160.
- Friston KJ, Ashburner J, Frith C, Poline J, Heather J, Frackowiak R (1995a) Spatial registration and normalization of images. *Hum Brain Mapp* 2:165–189.
- Friston KJ, Holmes AP, Worsley KJ, Poline JP, Frith CD, Frackowiak RSJ (1995b) Statistical parametric maps in functional imaging: a general linear approach. *Hum Brain Mapp* 2:189–210.
- Friston KJ, Holmes A, Poline JB, Price CJ, Frith CD (1996) Detecting activations in PET and fMRI: levels of inference and power. *NeuroImage* 4:223–235.
- Fu QG, Flament D, Coltz JD, Ebner TJ (1997) Relationship of cerebellar Purkinje cell simple spike discharge to movement kinematics in the monkey. *J Neurophysiol* 78:478–491.
- Fukushima K, Fukushima J, Kaneko CR, Fuchs AF (1999) Vertical

- Purkinje cells of the monkey floccular lobe: simple-spike activity during pursuit and passive whole body rotation. *J Neurophysiol* 82:787–803.
- Galambos R, Makeig S, Talmachoff PJ (1981) A 40-Hz auditory potential recorded from the human scalp. *Proc Natl Acad Sci USA* 78:2643–2647.
- Griffiths TD (2000) Musical hallucinosis in acquired deafness: phenomenology and brain substrate. *Brain* 123:2065–2076.
- Gutschalk A, Mase R, Roth R, Ille N, Rupp A, Hahnel S, Picton TW, Scherg M (1999) Deconvolution of 40 Hz steady-state fields reveals two overlapping source activities of the human auditory cortex. *Clin Neurophysiol* 110:856–868.
- Hirano S, Naito Y, Okazawa H, Kojima H, Honjo I, Ishizu K, Yenokura Y, Nagahama Y, Fukuyama H, Konishi J (1997) Cortical activation by monaural speech sound stimulation demonstrated by positron emission tomography. *Exp Brain Res* 113:75–80.
- Johnson BW, Weinberg H, Ribary U, Cheyne DO, Ancill R (1988) Topographic distribution of the 40 Hz auditory evoked-related potential in normal and aged subjects. *Brain Topogr* 1:117–121.
- Kapoor R, Griffin G, Barrett G, Fowler CJ (1991) Myoclonic epilepsy in an HIV positive patient: neurophysiological findings. *Electroencephalogr Clin Neurophysiol* 78:80–84.
- Kiehl KA, Laurens KR, Duty TL, Forster BB, Liddle PF (2001) Neural sources involved in auditory target detection and novelty processing: an event-related fMRI study. *Psychophysiology* 38:133–142.
- Lockwood AH, Salvi RJ, Coad ML, Arnold SA, Wack DS, Murphy BW, Burkard RF (1999) The functional anatomy of the normal human auditory system: responses to 0.5 and 4.0 kHz tones at varied intensities. *Cereb Cortex* 9:65–76.
- Maiste AC, Wiens AS, Hunt MJ, Scherg M, Picton TW (1995) Event-related potentials and the categorical perception of speech sounds. *Ear Hear* 16:68–90.
- Makela JP, Hari R (1987) Evidence for cortical origin of the 40 Hz auditory evoked response in man. *Electroencephalogr Clin Neurophysiol* 66:539–546.
- Marple-Horvat DE, Criado JM, Armstrong DM (1998) Neuronal activity in the lateral cerebellum of the cat related to visual stimuli at rest, visually guided step modification, and saccadic eye movements. *J Physiol (Lond)* 506:489–514.
- Oldfield RC (1971) The assessment and analysis of handedness: the Edinburgh inventory. *Neuropsychologia* 9:97–113.
- Pantev C, Roberts LE, Elbert T, Ross B, Wienbruch C (1996) Tonotopic organization of the sources of human auditory steady-state responses. *Hear Res* 101:62–74.
- Parra J, Kalitzin S, Blanes W, Kasteleijn-Nolst Trenité D, Lopes da Silva F (2001) Stimulus-induced MEG gamma band synchronization in photosensitive epilepsy. *Ann Neurol* 50:S47.
- Penhune VB, Zatorre RJ, Evans AC (1998) Cerebellar contributions to motor timing: a PET study of auditory and visual rhythm reproduction. *J Cogn Neurosci* 10:752–765.
- Picton TW, Vajsar J, Rodriguez R, Campbell KB (1987) Reliability estimates for steady-state evoked potentials. *Electroencephalogr Clin Neurophysiol* 68:119–131.
- Portas CM, Krakow K, Allen P, Josephs O, Armony JL, Frith CD (2000) Auditory processing across the sleep-wake cycle: simultaneous EEG and fMRI monitoring in humans. *Neuron* 28:991–999.
- Ramnani N, Toni I, Josephs O, Ashburner J, Passingham RE (2000) Learning- and expectation-related changes in the human brain during motor learning. *J Neurophysiol* 84:3026–3035.
- Santarelli R, Maurizi M, Conti G, Ottaviani F, Paludetti G, Pettorossi VE (1995) Generation of human auditory steady-state responses (SSRs). II. Addition of responses to individual stimuli. *Hear Res* 83:9–18.
- Schmahmann JD, Pandya DN (1991) Projections to the basis pontis from the superior temporal sulcus and superior temporal region in the rhesus monkey. *J Comp Neurol* 308:224–248.
- Schmahmann JD, Doyon J, McDonald D, Holmes C, Lavoie K, Hurwitz AS, Kabani N, Toga A, Evans A, Petrides M (1999) Three-dimensional MRI atlas of the human cerebellum in proportional stereotaxic space. *NeuroImage* 10:233–260.
- Steriade M, Dossi RC, Pare D, Oakson G (1991) Fast oscillations (20–40 Hz) in thalamocortical systems and their potentiation by mesopontine cholinergic nuclei in the cat. *Proc Natl Acad Sci USA* 88:4396–4400.
- Strahlendorf JC, Lee M, Strahlendorf HK (1984) Effects of serotonin on cerebellar Purkinje cells are dependent on the baseline firing rate. *Exp Brain Res* 56:50–58.
- Talairach J, Tournoux P (1988) Co-planar stereotaxic atlas of the human brain. New York: Thieme.
- Tijssen MA, Thom M, Ellison DW, Wilkins P, Barnes D, Thompson PD, Brown P (2000) Cortical myoclonus and cerebellar pathology. *Neurology* 54:1350–1356.
- Ugawa Y, Day BL, Rothwell JC, Thompson PD, Merton PA, Marsden CD (1991) Modulation of motor cortical excitability by electrical stimulation over the cerebellum in man. *J Physiol (Lond)* 441:57–72.
- Zatorre RJ, Evans AC, Meyer E, Gjedde A (1992) Lateralization of phonetic and pitch discrimination in speech processing. *Science* 256:846–849.